Session 3P4
Subsurface Imaging through Inverse Scattering Approaches: From Biomedical Applications to UXO Detection

Beam Manipulation of a Monopole Antenna

C. J. Fox, **P. M. Meaney**, **L. Potwin**, **and K. D. Paulsen**
Dartmouth College, USA

We are currently in the process of optimizing our microwave tomographic imaging system for the detection of breast cancer. One area targeted in our optimization efforts is the antenna design. In both tomographic and radar based imaging approaches a broad frequency band is desired. Higher imaging frequencies offer many advantages in the field of breast cancer detection, particularly in improved resolution [1]. A broad target antenna bandwidth of 500 MHz to 3 GHz allows us to analyze the most realistic maximum operating frequency in the actual clinical setting. Broadband capability is especially important for our image reconstruction algorithm which involves the use of a variance stabilizing transformation. This process requires simultaneous analysis of both the signal's magnitude and phase. The phase component poses significant challenges because of its wrapping characteristics and the broadband data is particularly useful in the unwrapping process [2].

There are two ways to generate broadband antennas. One technique involves making the antennas physically large, such as for spiral antennas. Alternatively, the antennas can be resistively loaded. Unfortunately, resistively loading an antenna reduces its efficiency dramatically [3]. Our current clinical system uses 16 monopole antennas submerged in a lossy coupling liquid. We have addressed the loss of antenna efficiency by creating a tomographic system with a large dynamic range and a small target zone. Antennas used in breast cancer imaging systems need to be small as well as operate over a broad frequency range. The resistively loaded coaxial monopole easily satisfies the tight space requirements of breast imaging and has a sufficiently broad frequency range. Additionally, the monopole antenna's beam pattern is isotropic in the dorsal imaging plane.

Even though the beam pattern is isotropic in the imaging plane the orthogonal distribution of the beam is not necessarily centered. Measurements show that the beam narrows and steers upward with increasing frequency. The upward steering of the beam leads to an increase in signal coupling to surface modes which create unwanted multi-path signals. We have undertaken a thorough analysis of this behavior and discussed a strategy for extending the use of these antennas to the full frequency range. We will show a summary of this analysis and an optimized antenna design. We will also show images at higher frequencies made possible by our design optimizations.

*This work was supported by NIH/NCI grant # R01 CA80139.

REFERENCES

1. Fear, E. C., S. C. Hagness, P. M. Meaney, M. Okoniewski, and M. A. Stuchly, "Enhancing breast tumor detection with nearfield imaging," *IEEE Microwave Mag.*, Vol. 3, No. 1, 48–56, Mar. 2002.
2. Meaney, P. M., Q. Fang, M. W. Fanning, T. Raynolds, P. Robbie, and K. D. Paulsen, "Microwave imaging using the adjoint method: facilitating advances in software and hardware development," *2nd International Conference on Electromagnetic Near-Field Characterization and Imaging*, Barcelona, Spain, 67–71, June, 2005.
3. Yin, X., E. C. Fear, and R. H. Johnston, "Compact antenna for radar-based breast cancer detection," *IEEE Trans. on Antennas and Propagation*, Vol. 53, No. 8, 2374–2380, August 2005.

Iterative Reconstruction of Dielectric Rough Surface Profiles through a Single Illumination

I. Akduman[1], R. Kress[2], and A. Yapar[1]

[1]Istanbul Technical University, Turkey
[2]University of Goettingen, Germany

Imaging of an inaccessible rough surface constitutes an important class of problems in inverse scattering theory due to the large domain of applications such as microwave remote sensing, underground imaging, optical system measurements, underwater acoustics, non-destructive testing etc. In these kinds of problems one tries to recover the location and shape, as well as the surface characteristics of an unknown surface through scattered field measurements in a certain domain. The surface to be reconstructed may be either a perfectly conduction one or a dielectric interface separating two-dielectric media. As far as we know several exact and numerical techniques have been developed for perfectly conducting surfaces, where most of these inversion schemes are concerned with the reconstruction of surfaces with small perturbations. On the other hand reconstruction of a rough dielectric interface is of importance in the practical applications since most of the boundaries in nature are surfaces separating dielectric mediums. Recently little progress has been done for solving this challenging problem [1–3].

In this paper, we give a new, simple and fast method to determine the location and shape of a rough surface separating two lossy dielectric half-spaces. For the sake of simplicity, we consider surfaces having a variation in one direction. The reconstruction is achieved via a single illumination of a plane wave at a fixed frequency and the reflected field measurements are performed on a line parallel to the mean surface. In the method presented here the lossy half-space above the surface is first separated into two parts by a certain plane, and then the scattered field in the upper region above this plane is expressed in terms of a Fourier transform while it is expanded into a Taylor series in the lower part. Similar representation is used for the scattered field in the half-space below the surface. The use of the continuity conditions of the total field and its derivative on the unknown surface allows the reduction of the problem to the solution of a coupled system of equations containing a spectral coefficient for the scattered field and the surface function as unknowns. The coupled system is solved iteratively starting from an initial guess of the surface function, i.e.: for a given initial estimate of the surface profile one of the equations which is linear and ill-posed is solved for the spectral coefficient of the scattered field through Tikhonov regularization. Then one inserts this solution in the other equation which is non-linear and linearize it in the Newton sense and so on. Since the solution is sensitive to the errors in data, a regularization in the least square sense is applied in the Newton iteration scheme. The method yields satisfactory reconstructions for slightly varying surface profiles.

REFERENCES

1. Stankova, M., J. Burov, and M. Burova, "Computer reconstruction of a periodic surface by means of the scattered and transmitted acoustic fields," *Measurements Sci. and Tech.*, Vol. 12, 1330–1335, 2001.
2. Galdi, V., J. Pavlovich, W. C. Karl, D. A. Castanon, and L. B. Felsen, "Moderately rough dielectric interface profile reconsruction via short-pulse quasi-ray Gaussian beams," *IEEE Trans. Antennas and Propagation*, Vol. 51, No. 3, 672–677, 2003.
3. El-Shenawee, M. and E. L. Miller, "Multiple-incidence and multifrequency for profile reconstruction of of random rough surfaces using the 3-D electromagnetic fast multipole model," *IEEE Trans. Geoscience and Remote Sensing*, Vol. 42, No. 11, 2499–2510, November 2004.

The Semi-analytic Mode Matching (SAMM) Algorithm for Fast Computation of Scattered Near Fields from a Variety of Dielectric Targets Buried in Lossy Soil Excited by Underground Borehole Dipole Sources

A. W. Morgenthaler and C. Rappaport
Northeastern University, USA

The 3D semi-analytic mode matching (SAMM) algorithm is used to determine the near field scattering of dipole sources from a variety of 2D or 3D underground targets with complex dielectric constants, extending previous work with uniform plane wave sources. The dipole sources may be located above ground, useful for modeling forward GPR scattering of buried targets like landmines, or below ground which is more useful for simulating cross borehole tomography used to locate and identify pollution pools or for general geophysical sensing.

Scattering is described by moderately low-order superpositions of 2D cylindrical modes or 3D spherical modes, each originating from user-specified coordinate scattering centers (CSCs). The CSCs are chosen where scattering appears to originate, including within the target (multiple CSCs may be required if the target deviates substantially from a quasi-spherical shape), at the source image, and at the above-ground images which model backscatter from the lossy ground surface into the ground region. The mode coecients are found numerically by least-squares fitting all boundary conditions at discrete points along the relevant air-ground and ground-target interfaces. The optimal distribution of fitting points along these interfaces is also discussed. For a favorable choice of CSCs and a careful selection of fitting points, the SAMM algorithm converges with increasing mode number, giving rise to accurate scattering fields in a time 2-3 orders of magnitude faster than FDFD simulations. SAMM can thus be used as a forward model for inverse scattering algorithms, giving them the ability to find buried objects quickly.

*This work is supported by CenSSIS, the Center for Subsurface Sensing and Imaging Systems under the ERC Program of the NSF (Award number EEC-9986821).

Recent Advances on the Use of Kernel-based Learning-by-examples Techniques for Electromagnetic Subsurface Sensing

M. Benedetti, **M. Donelli**, **D. Franceschini**, **A. Rosani**, **A. Boni**, **and A. Massa**
University of Trento, Italy

To return areas contaminated with unexploded ordnance (UXO) and anti-tank/anti-personnel landmines to a civilian use, the ordnances should be obviously removed. Such a process is time-expensive and involves complex acquisition procedures. Several solutions have been proposed based on various methodological approaches, which consider different sensor modalities such as ground-sensors or synthetic aperture radars. These techniques are aimed at achieving the following goals: (a) correctly localizing a large number of dangerous targets; (b) reducing the false-alarm rate; (c) reducing the time devoted to the detection process. In such a framework, electromagnetic approaches based on learning-from-samples (LFS) techniques [1] have been proposed for the on-line (after the training phase performed off-line) detection of subsurface objects. The detection process is recast as a regression problem where the unknowns (i.e., geometric and dielectric characteristics of the target) are evaluated from the data (i.e., the value of the scattered field) by approximating the data-unknowns relation through an off-line data fitting process (training). LFS regression-based approaches demonstrated their effectiveness in dealing with detection processes where a limited number of unknowns (i.e., single object) is considered. However, because of the complexity of the underlying architecture, some difficulties occur when a larger number of unknowns (i.e., multiple objects) is taken into account. From a structural point-of-view, the regression technique does not permit one to simultaneously identify multiple positions. As a consequence, LFS regression-based approaches turn out to be very effective for the detection of a single (or few organized in a single cluster of objects) buried object. It should be pointed out that the identification of free-areas and an estimate of the concentration of subsurface objects might be enough in several situations. Then, the goal could be moved from the "*object detection*" to the "*definition of a risk map*" [2]. Consequently, a classification approach, instead of a regression one, should be employed. In this contribution, the classification approach based on a LFS technique preliminary presented in [3] for an on-line sub-surface sensing is analysed and compared to state-of-the-art classification approaches. Starting from the knowledge of the scattered field values collected above the surface, the method is aimed at defining a risk map of the domain under test. By considering a SVM-based classifier, the proposed method estimates the a-posteriori probability of the presence of subsurface dangerous objects. The advantages of the use of such an instance-based classification method can be summarized as follows: (a) no *a-priori* knowledge about the system that generated the data is required; (b) simplicity and reliability of the resolution algorithm; (c) possibility of designing optimal classifier based on the theory by *Vapnik and Chervonenkis*; (d) easy implementation in hardware for real-time applications.

REFERENCES

1. Bermani, E., A. Boni, S. Caorsi, and A. Massa, "An innovative real-time technique for buried object detection," *IEEE Trans. on Geoscience and Remote Sensing.*, Vol. 41, 927–931, Apr. 2003.
2. Caorsi, S., E. Bermani, A. Boni, M. Conci, M. Donelli, and A. Massa, "Learning-by-examples strategies for sub-surface imaging: from regression to classification approach," *PIERS2003*, USA, 118, Oct. 2003.
3. Caorsi, S., E. Bermani, A. Boni, M. Donelli, and A. Massa, "On the effectiveness of kernel-based learning-by-examples techniques for electromagnetic subsurface sensing," *PIERS2004*, Italy, S3.02, Mar. 2004.

Application of Spheroidal Mode Approach to the Detection and Discrimination of Buried Objects

X. D. Chen[1], **K. O'Neill**[2], **T. M. Grzegorczyk**[3], **and J. A. Kong**[3]

[1]National University of Singapore, Singapore
[2]ERDC Cold Regions Research and Engineering Laboratory, USA
[3]Massachusetts Institute of Technology, USA

The detection and removal of buried unexploded ordnance (UXO) is an important environmental problem, made very expensive and challenging by the high false alarm rate. Among the techniques for detecting UXOs, electromagnetic induction (EMI) is promising and has been widely explored. In the magneto-quasistatic (MQS) regime, both the primary and the secondary magnetic fields are irrotational and can be expressed in terms of the gradient of a scalar potential governed by the Laplace equation. In this work, both the primary and the secondary magnetic fields are expressed as linear superpositions of basic modes in the spheroidal coordinate system. Spheroidal modes are chosen because the spheroidal coordinate system can be made to conform to the general shape of an object of interest, whether flattened or elongated, and many of our objects of interest are bodies of revolution. Due to the orthogonality and the completeness of the spheroidal basic modes, the scattering coefficients, in response to unitary magnitude of the primary mode excitation, are uniquely determined. They are characteristics of the object and can then be treated as discriminators in pattern matching and classification. The scattering coefficients are retrieved from the knowledge of the secondary fields, where both the synthetic and measurement data are used. The ill-conditioning issue is dealt with by mode truncation and Tikhonov regularization technique. Stored in a library, the scattering coefficients can produce fast forward models for use in pattern matching. Also they can be used to train a support vector machine (SVM) to sort objects into generic classes, such as elongated or not, permeable or not. The success of the retrieval from both synthetic and measurement data shows the promise of the spheroidal mode approach in the detection and classification of buried objects.

Subsurface Estimation of the Geometry and Electromagnetic Properties of Buried Anomaly and Half-space Background with Unknown Rough Boundary

R. Firoozabadi, E. L. Miller, C. Rappaport, and A. W. Morgenthaler
Northeastern University, USA

A new inverse method is developed to recover the geometric structure and electromagnetic contrast of an anomaly buried in a half-space defined by a rough, unknown boundary. Spline curves are used to model both the shape of the object as well as the profile of the boundary. The problem is then cast as one of determining a relatively small number of control points for these curves along with the complex permittivities of the anomaly and the background medium. The direct relationship between the control points and the boundary points and nonlinear relationship between the geometry and resulting scattered field defined by Maxwell's equations enable us to restore these parameters with a high degree of accuracy even when the data are corrupted by noise.

The physical forward model employed in the inversion algorithm is the Semi-Analytic Mode Matching method (SAMM) which is a fast and efficient method to calculate the scattered near-fields from a buried lossy homogenous object in the lossy homogenous background and is defined in terms of the modal expansions enforcing the boundary conditions at the boundaries of different media. SAMM is of low computational complexity compared to other methods and highly accurate in the region of interest.

The Levenberg-Marquardt method is used as a nonlinear least-squares minimization algorithm to optimize the unknown parameters including the control points and complex permittivities. In the talk accompanying this abstract we provide details concerning the manner in which the SAMM model allows us to compute closed form expressions for the sensitivity of the scattered fields with respect to both the geometric and contrast parameters. Numerical results will be provided to verify the capability of the proposed algorithm.

REFERENCES

1. Morgenthaler, A. W. and C. M. Rappaport, "Scattering from dielectric objects buried beneath randomly rough ground: Validating the semi-analytic mode matching algorithm with 2-D FDFD," *IEEE Trans. Geoscience and Remote Sensing*, Vol. 39, 2421–2428, November 2001.
2. Firoozabadi, R., E. L. Miller, C. M. Rappaport, and A. W. Morgenthaler, "New inverse method for simultaneous reconstruction of object buried beneath rough ground and the ground surface structure using SAMM forward model," *IS&T/SPIE 17th Annual Symposium on Electronic Imaging: Science and Technology*, 382–393, San Jose, CA, 16–20 January 2005.

The Adjoint-field Method for Reconstructing Breast Cancer Tumors of Irregular Shape

M. El-Shenawee[1], **O. Dorn**[2], **and M. Moscoso**[2]

[1]University of Arkansas, USA
[2]Universidad Carlos III de Madrid, Spain

In this work we combine the method of moments for 3D electromagnetic propagation and the adjoint field method for shape reconstruction for the problem of breast tumor detection using microwaves. The method of moments forward solver is used to calculate the scattered fields at several receivers surrounding the tumor. Moreover, the total fields are calculated everywhere in the considered domain including the interface of the tumor. The mismatch between calculated and synthetically measured fields is then used as new sources at all receiver locations and is back-propagated towards the tumor by just solving another forward problem with the method of moments code. The gradient is calculated as the product of the forward and adjoint fields at the best guess of the tumor interface in order to extract a new search direction. The location of each surface node is then updated individually based on these new gradient values in the normal direction of the surface. Using this technique, the forward solver will be used only twice, regardless of the shape of the tumor; once for solving the forward problem and once for the adjoint problem. This process is repeated iteratively until the mismatch in the data is minimized according to some criterion.

In our previous work, the irregular shape of a malignant tumor was modeled using a spherical harmonics representation, which leads to smooth reconstructions. However, sometimes it is desirable to be able to recover more irregular shapes, which cannot be achieved efficiently by the spherical harmonics method. Therefore, we will use in this work a more general representation directly given by the discretization mesh of the method of moments. Doing so, we need to find an efficient way for calculating shape gradients. Instead of using the often employed perturbative method for this purpose, we will use an adjoint field method which is more efficient in this situation.

In our numerical experiments, the background medium is assumed to be homogeneous and lossy. The embedded tumors are assumed to be shape-like with constant dielectric parameters inside. The contrast in these dielectric parameters between tumors and background medium is assumed to be high, which is typical for breast tumors. We will present several numerical results in 3D based on the proposed technique using multiple transmitting sources/receivers at multiple microwave frequencies.

Nonlinear Inversion of Multi-frequency Microwave Fresnel Data Using the Multiplicative Regularized Contrast Source Inversion

A. Abubakar and T. M. Habashy
Schlumberger-Doll Research, USA

P. M. van den Berg
Delft University of Technology, The Netherlands

Abstract—This paper presents the results of profile inversion of multi-frequency electromagnetic scattered field data, measured by the Institute Fresnel, Marseille, France, from cylindrical objects, both for TM and TE illuminations. The reconstructions are obtained by applying the Multiplicative Regularized Contrast Source Inversion (MR-CSI) method. The results show that the MR-CSI method successfully performs 'blind' inversion of a wide class of scattered field data. Further, we also show that by inverting both TM and TE data simultaneously, a more accurate reconstructed image can be obtained.

1. Introduction

We discuss the performance of the Contrast Source Inversion (CSI) method [1, 2], enhanced with a Multiplicative Regularization technique (MR-CSI) [3]. The MR-CSI method has been applied to invert the first set of data measured by the Institut Fresnel, Marseille, France [4]. The inversion results obtained using the MR-CSI method from these first Fresnel data sets were presented in [5]. Following these experiments, the MR-CSI method has been improved by the introduction of the so-called weighted L_2-norm regularizer, see [6]. The inversion results of the first Fresnel data set using the MR-CSI method with weighted L_2-norm regularizer can be found in [7].

With this version of the MR-CSI method we demonstrate the reconstructions from the second set of data measured by the Institut Fresnel. We carry out a 'blind' inversion of these data sets without explicitly taking into consideration any *a priori* information regarding the type of objects (either dielectric or metallic) to be reconstructed. In all cases we reconstruct both the permittivity and the conductivity of the unknown objects. The only *a priori* information which is used in the inversion is the positivity constraint on both permittivity and conductivity. The inversion results show that the MR-CSI method seems to handle the experimental field data very well. Furthermore we will show that by inverting both TM and TE data simultaneously we are able to arrive at more accurate reconstructed images.

2. Methodology

The Institute Fresnel experimental setup consists of a transmitting and a receiving antennas, both of which are double-ridged horn antennas. The antennas are moved on a circular rail around the object(s). The objects are elongated in the direction perpendicular to the plane in which the antennas are rotated (i. e., the plane of measurement), that a two-dimensional (2D) model is appropriate. In the plane of illumination, we choose a 2D rectangular test domain D containing the object(s). The transmitting antenna illuminates the objects from different locations distributed equidistantly around the object. We use the subscript j to denote the measured frequency and the subscript s to denote the dependence on the transmitter position. The receiving antenna measures the total field and the incident field from a number of different locations distributed equidistantly around the object. The scattered field, which is needed in the inversion, can then be found by subtracting the incident field from the total field.

The experimental data are collected at a number of frequencies with time factor $\exp(-i\omega_j t)$ where $i^2 = -1$, ω_j is the radial frequency and t is time. We introduce the vectors $\boldsymbol{p}$ and $\boldsymbol{q}$ as the spatial positions in 2D. We use the Maxwell model for the constitutive parameters of the object. Hence the contrast function for each frequency is defined as follows:

$$\chi_j(\boldsymbol{q}) = \frac{\varepsilon(\boldsymbol{q}) - \varepsilon_0}{\varepsilon_0} + i\frac{\sigma(\boldsymbol{q})}{\omega_j \varepsilon_0}, \tag{1}$$

where ε and σ denote the permittivity and conductivity, which are frequency independent. The symbol ε_0 denotes the permittivity in vacuum. Since ε and σ are frequency independent, it is obvious that in the inversion we need only to invert for one value of the contrast function. Let χ_1 be the contrast function value at the angular frequency ω_1, then the other values of the contrast as a function of frequency can be calculated through:

$$\chi_j(\boldsymbol{q}) = \mathrm{Re}[\chi_1(\boldsymbol{q})] + i\frac{\omega_1}{\omega_j}\mathrm{Im}[\chi_1(\boldsymbol{q})]. \tag{2}$$

Since all the objects lie inside a test domain D, the contrast function is therefore non-zero inside D and zero elsewhere.

In the $TM-case$ where the non-zero component of the electric field is the only one parallel to the cylindrical objects, we deal with a scalar wave field problem. The domain integral representation for the scattered field as a function of the total field u_s, j and the contrast χ_j is given by

$$u^{sct}_{s,j}(\boldsymbol{p}) = K^{TM}_j[\chi_j u_{s,j}] = k^2_{0,j}\int_D g_j(\boldsymbol{p},\boldsymbol{q})\chi_j(\boldsymbol{q})u_{s,j}(q)\mathrm{dv}(\boldsymbol{q}), \quad \boldsymbol{p}\in S, \tag{3}$$

where $k_{0,j} = \omega_j\sqrt{\varepsilon_0\mu_0}$ is the wave number in free-space and S is the data domain where the transmitter and receiver are located. The scalar homogeneous Green function is given by

$$g_j(\boldsymbol{p},\boldsymbol{q}) = \frac{i}{4}H^{(1)}_0(k_{0,j}|\boldsymbol{p}-\boldsymbol{q}|), \tag{4}$$

where $H^{(1)}_0$ denotes the first kind Hankel function of zero order.

In the $TE-case$, the field quantities are two-components vectors representing the electric field components in the transversal plane of the cylindrical objects. The domain integral representation for the scattered field vector as a function of the total field $\boldsymbol{u}_{s,j}$ and the contrast χ_j is given by

$$\boldsymbol{u}^{sct}_{s,j}(\boldsymbol{p}) = K^{TE}_j[\chi_j\boldsymbol{u}_{s,j}] = (k^2_{0,j}+\nabla\nabla\cdot)\int_D g_j(\boldsymbol{p},\boldsymbol{q})\chi_j(\boldsymbol{q})\boldsymbol{u}_{s,j}(\boldsymbol{q})\mathrm{dv}(\boldsymbol{q}), \quad \boldsymbol{p}\in S, \tag{5}$$

where ∇ is the spatial differentiation operator with respect to $\boldsymbol{p}$.

The TM and TE total field, and the contrast inside the test domain D satisfy the following integral equation:

$$u^{inc}_{s,j}(\boldsymbol{p}) = u_{s,j}(\boldsymbol{p}) - K^{TM}_j[\chi_{j,n}u_{s,j,n}], \quad \boldsymbol{u}^{inc}_{s,j}(\boldsymbol{p}) = \boldsymbol{u}_{s,j}(\boldsymbol{p}) - K^{TE}_j[\chi_{j,n}\boldsymbol{u}_{s,j,n}], \quad \boldsymbol{p}\in D \tag{6}$$

where the operators $K^{TM}_j[\chi_j u_{s,j}]$ and $K^{TE}_j[\chi_j\boldsymbol{u}_{s,j}]$ are defined in (3) and (5), for the TM-case and TE-case respectively. Eqs. (3), (5) and (6) are the basic equations for developing any inversion algorithm based on the integral equation formulation. The goal of solving the inverse scattering problem can be formulated as follows: Solve (3) or (5) to obtain the contrast χ_1 on D from the knowledge of the scattered field $u^{sct}_{s,j}$ on S and the incident field $u^{inc}_{s,j}$ on D subject to the necessary condition that the total field $u_{s,j}$ on D and the contrast χ_1 on D satisfy the integral equation in (6).

We consider the inverse scattering problem as an optimization problem where, in each iteration n, we update the contrast sources $w_{s,j,n} = \chi_j u_{s,j,n}$ and the contrast $\chi_{j,n}$ alternatingly, by minimization of the cost function. For the TM inversion the cost function is given by

$$F_n(\chi_{1,n}, w_{s,j,n}) = \left[\frac{\sum_{s,j}\|u^{sct}_{s,j} - K^{TM}_j[w_{s,j,n}]\|^2_S}{\sum_{s,j}\|u^{sct}_{s,j}\|^2_S} + \frac{\sum_{s,j}\|w_{s,j,n} - \chi_{j,n}u_{s,j,n}\|^2_D}{\sum_{s,j}\|\chi_{j,n-1}u^{inc}_{s,j}\|^2_D}\right]\int_D \frac{|\chi_{1,n}(\boldsymbol{p})|^2+\delta^2_n}{|\chi_{1,n-1}(\boldsymbol{p})|^2+\delta^2_n}\mathrm{dv}(\boldsymbol{p}), \tag{7}$$

where

$$u_{s,j,n} = u^{inc}_{s,j} + K^{TM}_j[w_{s,j,n}], \quad \delta^2_n = \frac{1}{\Delta^2}\frac{\sum_{s,j}\|w_{s,j,n-1} - \chi_{j,n-1}u_{s,j,n-1}\|^2_D}{\sum_{s,j}\|\chi_{j,n-1}u^{inc}_{s,j}\|^2_D} \tag{8}$$

and $\|\cdot\|^2_S$ and $\|\cdot\|^2_D$ denote the L_2-norm on the data domain S and the object domain D, respectively. The symbol Δ denotes the mesh size of the discretization grid. In this CSI method, we use the back-propagation step to arrive at initial estimates for the contrast sources and the contrast. After the initial step, in each iteration the contrast sources and the contrast are updated alternatingly each by using one conjugate gradient step. The optimization process may be terminated if one of the following stopping conditions is satisfied:

- The difference between the normalized data error F_n at two successive iterates, n-th and $(n-1)$-th, is within a prescribed error quantity (it set to be 10^{-5}).

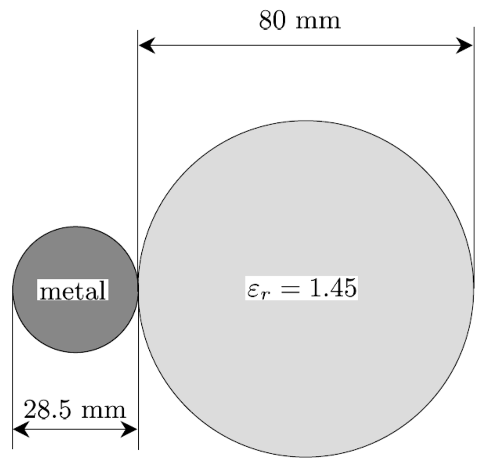

Figure 1: The configuration used to obtain the data sets FoamMetExtTM.exp and FoamMetExtTE.exp.

- The total number of iterations exceeds a prescribed maximum N_{max}=512.

The *a priori* information that the permittivity and the conductivity are positive are implemented by enforcing the negative value to zero after each iteration. This simple procedure is employed in all of the inversion runs. Details of this so-called MR-CSI method for multi-frequency problem can be found in [5]. However the procedure to update the contrast function is replaced by the improved version in [7]. For the TE inversion the cost function in (7) is replaced by

$$F_n(\chi_{1,n},\boldsymbol{w}_{s,j,n})=\left[\frac{\sum_{s,j}\|\boldsymbol{u}^{sct}_{s,j}-K^{TE}_j[\boldsymbol{w}_{s,j,n}]\|^2_S}{\sum_{s,j}\|\boldsymbol{u}^{sct}_{s,j}\|^2_S}+\frac{\sum_{s,j}\|\boldsymbol{w}_{s,j,n}-\chi_{j,n}\boldsymbol{u}_{s,j,n}\|^2_D}{\sum_{s,j}\|\chi_{j,n-1}\boldsymbol{u}^{inc}_{s,j}\|^2_D}\right]\int_D\frac{|\chi_{1,n}(\boldsymbol{p})|^2+\delta^2_n}{|\chi_{1,n-1}(\boldsymbol{p})|^2+\delta^2_n}\mathrm{dv}(\boldsymbol{p}), \quad (9)$$

where

$$u_{s,j,n}=u^{inc}_{s,j}+K^{TE}_j[w_{s,j,n}]. \quad (10)$$

Further, for joint TM and TE data inversion, the cost function to be minimized is given by

$$\begin{aligned}F_n(\chi_{1,n},w_{s,j,n},\boldsymbol{w}_{s,j,n}) \;=\; &\left[\frac{\sum_{s,j}\|u^{sct}_{s,j}-K^{TM}_j[w_{s,j,n}]\|^2_S}{\sum_{s,j}\|u^{sct}_{s,j}\|^2_S}+\frac{\sum_{s,j}\|w_{s,j,n}-\chi_{j,n}u_{s,j,n}\|^2_D}{\sum_{s,j}\|\chi_{j,n-1}u^{inc}_{s,j}\|^2_D}\right.\\ &\left.+\frac{\sum_{s,j}\|\boldsymbol{u}^{sct}_{s,j}-K^{TE}_j[\boldsymbol{w}_{s,j,n}]\|^2_S}{\sum_{s,j}\|\boldsymbol{u}^{sct}_{s,j}\|^2_S}+\frac{\sum_{s,j}\|\boldsymbol{w}_{s,j,n}-\chi_{j,n}\boldsymbol{u}_{s,j,n}\|^2_D}{\sum_{s,j}\|\chi_{j,n-1}\boldsymbol{u}^{inc}_{s,j}\|^2_D}\right]\\ &\int_D\frac{|\chi_{1,n}(\boldsymbol{p})|^2+\delta^2_n}{|\chi_{1,n-1}(\boldsymbol{p})|^2+\delta^2_n}\mathrm{dv}(\boldsymbol{p}). \end{aligned} \quad (11)$$

3. Numerical Results

In this proceeding paper we only show the inversion results of the data sets FoamMetExtTM.exp and FoamMetExtTE.exp. The inversion results of other data sets will be presented during the conference. These data sets FoamMetExtTM.exp and FoamMetExtTE.exp are obtained by measuring a configuration as shown in Fig. 1. This configuration consists of one circular dielectric cylinder with a relative permittivity value of $\varepsilon_r = 1.45$ with a diameter of 80 mm and one metallic cylinder with a diameter of 28.5 mm. In the experiment, there are 18 transmitters distributed uniformly on a circle with a radius of 1.67 m from the center of the experimental setup. For each transmitter the data are measured using 241 receivers located on a circle with a radius of 1.67 m. The data are collected at 17 frequencies in the range of 2–18 GHz. In the experimental setup the fields are generated and received by horn antennas. However as we previously argued, the problem is predominantly 2D. Hence both receivers and transmitters are approximated as line receivers and line transmitters. Therefore, we carry out the calibration procedure outlined in [5].

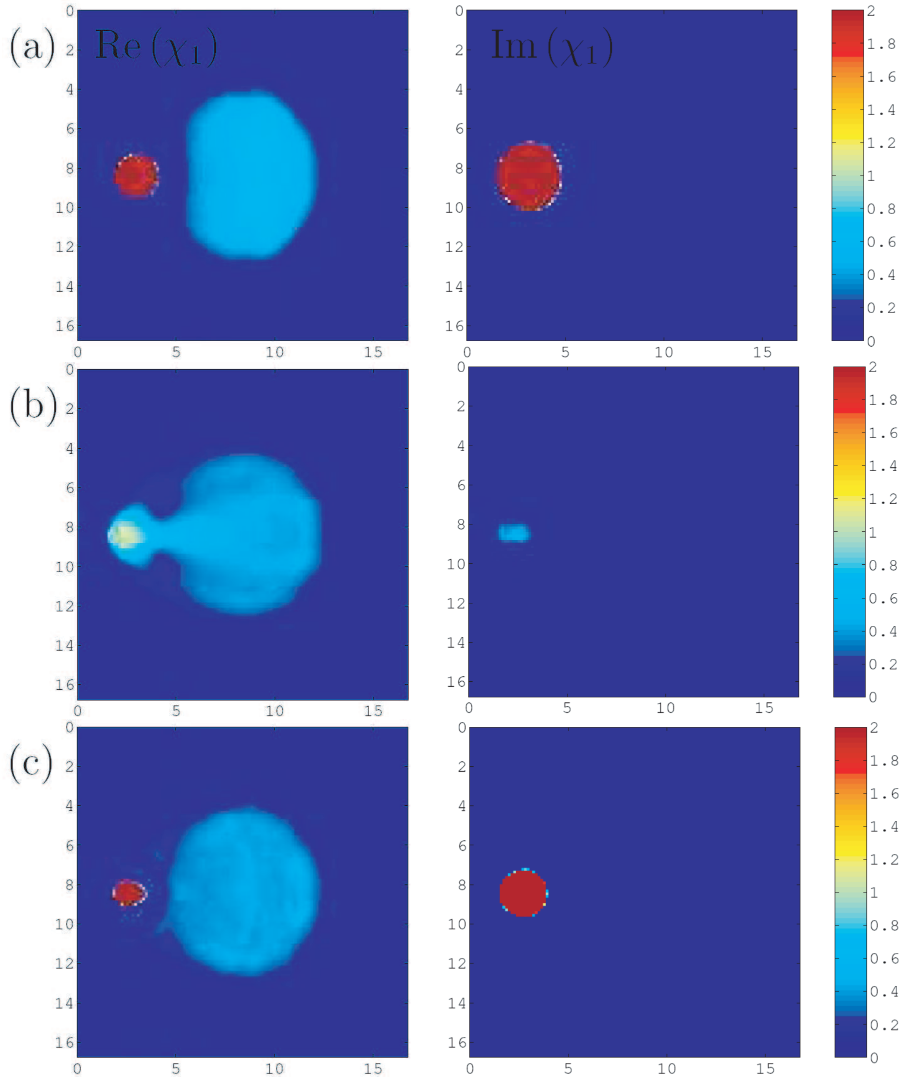

Figure 2: Reconstruction of the configuration with two disjoint cylinders, a dielectric one and a metallic one, for TM data polarization (data set: FoamMetExtTM.exp) (a) and TE data polarization (data set: FoamMetExtTE.exp) (b); and for joint inversion of both TM and TE data polarizations (c).

In the inversion we take a test domain D of 16.775 cm by 16.775 cm. The test domain D is discretized into 122 by 122 rectangular subdomains. The side length of each subdomain is 0.1375 cm. The wavelength at 18 GHz is 1.67 cm, hence the width and height of the test domain D is 10 time the wavelength in vacuum. The data for different frequencies are inverted simultaneously. However, in the figures we plot the complex contrast function χ_1 only. This is the complex contrast at the lowest frequency.

The reconstructed images from the TM and TE data sets are shown in Figs. 2(a) and (b). The left plots give the distribution of the real part of the reconstructed contrast function and while the right plots give the distribution of the imaginary part of the reconstructed contrast function. The inversion results from TM data set (see Fig. 2(a)) show that the metallic cylinder is retrieved with real and imaginary parts having the same order of magnitude. These inversion results also show that there is an ambiguity in the inversion. In principle, when carrying out the inversion of a perfectly conducting cylinder one can only reconstruct uniquely the boundary of the object. Inside the metal object the contrast sources are invisible, with the consequence that any contrast inside the object may be arbitrarily arrived at. The small circular object with a large permittivity value appearing in the image of Re(χ_1) is obviously an artefact of the inversion algorithm. However since the reconstructed circular object in Re(χ_1) lies completely inside the circular cylinder in Im(χ_1), one can conclude that we are dealing with a metallic object. On the other hand, the imaginary parts of the contrast of the

TE inversion do not exhibit any significant features (see Fig. 2(b)). However the shape of the large dielectric cylinder is better reconstructed using the TE inversion than the one using the TM inversion.

Next we invert both the TM and TE data simultaneously. The results of this joint inversion are given in Fig. 2(c). By inverting both TM and TE data simultaneously we obtain an improved reconstructed image of the large dielectric cylinder. Furthermore the small artefact in the image of $\mathrm{Re}(\chi_1)$ is obviously lied completely inside the circular cylinder in $\mathrm{Im}(\chi_1)$. Hence, we can conclude that by inverting both the TM and TE data simultaneously we can obtain more accurate reconstructed images than by inverting the TM and TE data sets separately.

4. Conclusions

In view of the present results and our crude approximation of the transmitting and receiving antennas, the Multiplicative Regularized Contrast Source Inversion method seems to be very robust and is capable of 'blindly' handling a wide class of inverse scattering problems. Finally we note that by inverting both TM- and TE-data simultaneously, we can obtain more accurate reconstructed images.

Acknowledgement

The authors wish to thank Dr. M. Saillard and Dr. K. Belkebir for providing their second set of experimental data as an objective test of our inversion algorithm.

REFERENCES

1. Habashy, T. M., M. L. Oristaglio, and A. T. de Hoop, "Simultaneous nonlinear reconstruction of two-dimensional permittivity and conductivity," *Radio Science*, Vol. 29, 1101–18, 1994.
2. Van den Berg, P. M. and R. E. Kleinman, "A contrast source inversion method," *Inverse Problems*, Vol. 13, 1607–20, 1997.
3. Van den Berg, P. M., A. L. van Broekhoven, and A. Abubakar, "Extended contrast source inversion," *Inverse Problems*, Vol. 15, 1325–44, 1999.
4. Belkebir, K. and M. Saillard, "Guest editors' introduction, special section: testing inversion algorithms against experimental data," *Inverse Problems*, Vol. 17, 1565–71, 2001.
5. Bloemenkamp, R. F., A. Abubakar, and P. M. van den Berg, "Inversion of experimental multi-frequency data using the contrast source inversion method," *Inverse Problems*, Vol. 17, 1611–22, 2001.
6. Abubakar, A., P. M. van den Berg, and J. J. Mallorqui, "Imaging of biomedical data using a multiplicative regularized contrast source inversion method," *IEEE Transactions on Microwave Theory and Techniques*, Vol. 50, 1761–71, 2002.
7. Van den Berg, P. M., A. Abubakar, and J. T. Fokkema, "Multiplicative regularization for contrast profile inversion," *Radio Science*, Vol. 38, 23.1–10, 2003.

Reconstruction of 3-D Dielectric Objects from Experimental Data in the Time Domain

T. Takenaka, **T. Tanaka**, **and H. Zhou**
Nagasaki University, Japan

Many nonlinear inversion techniques have been proposed for imaging high-contrast objects both in the frequency domain and in the time domain. Since the use of a broad-band pulse allows a large amount of information about unknown scattering objects than a single frequency scattering data, we have proposed a time-domain inverse scattering imaging technique, the forward-backward time-stepping (FBTS) method, to reconstruct the electrical parameter (the permittivity and conductivity) profiles of the scattering objects. We have also shown its effectiveness in several numerical simulations for inhomogeneous anisotropic as well as isotropic objects in the previous works.

This paper reports the 3-D reconstruction of the relative permittivity profile of an unknown object from the experimental data in the time domain. Eight antenna elements are placed equally spaced in a measurement circle. One of the antenna elements are used as a transmitting antenna and emits a pulsed wave. The scattered wave by the object is collected by the rest of them. Instead of using a pulse generator, we use a vector network analyzer which generates a stepped-frequency signal. The time domain representation of the scattering data is attained via the inverse Fourier Transform. All the transmission response $S_{ji}(j \neq i)$ between the ith transmitting antenna and the jth receiving antenna (i, $j = 1, 2 \ldots, 8$) are measured. Then, we change the transmitter point to the next antenna point and repeat the same measurement until all the antenna positions are used as a transmitter point. Next we move the measurement circle in the vertical direction and continue the measurement in the same way. We change the height of the measurement circle twice, so that we get 168 scattered field data. These data S_{ji} are multiplied by the spectrum of an incident pulse. Then taking the inverse Fourier transform of the resultant spectrum, we get the time domain scattering data to apply the FBTS method to the reconstruction of the relative permittivity profile of the unknown object. The FBTS method was tested on the experimental data from a wooden hollow cylinder. The 3-D shape and the relative permittivity profile of the cylinder were successfully obtained.